Progress Report
to the
3rd J-PARC PAC Meeting

J-PARC E06 Experiment

Measurement of T-violating Transverse Muon Polarization in $K \to \pi^0 \mu^+ \nu$ Decays

E06 (TREK) Collaboration*

June 14, 2007†

*TREK is the acronym of "Time Reversal Experiment with Kaons". Contact person : J. Imazato (jun.imazato@kek.jp)

†An error in p.23 (the cost for the transfer of the spectrometer) was corrected on June 26, 2007.

Contents

1 Introduction

"The PAC would like the proponent to show that the improvement on the sensitivity and systematic uncertainty below 10^{-4} is attainable via detailed Monte Carlo studies, e.g. acceptance, B-field offset, detector misalignments and the new active polarimeter." This was the problem assignment given to us by the first PAC meeting in summer'06 together with the recommendation of stage-1 approval. These were very reasonable questions which should have been discussed in the proposal. Unfortunately, however, our Monte Carlo studies were not so well advanced at the submission of the proposal, and we could show only semi-quantitative arguments based on the analytical functions (of e.g. muon decay Michel spectrum) for the sensitivity estimate, and some conceptual methodology for the detector element alignment which plays the most essential role determining the systematic errors. In this report we answer these points.

One thing we should point out here is the follow-up explanation of the statement in the minutes concerning the statistical sensitivity. *"A 20-fold improvement (from E246) in the P_T (statistical) sensitivity requires"* not necessarily *"a 400-fold increase in statistics"*, but we are going to achieve the required sensitivity by *"an increase of the detector acceptance by a factor ten and an increase of 800 MeV/c K^+ beam flux by at least 30 times"* for one year's running with the help of substantial increase of the analyzing power. This point is also clarified in this report.

Monte Carlo studies can be very wide-ranging and diverse. In order to approach the problem by not losing essential points, we took the strategy to concentrate on the most crucial points both in the sensitivity estimate and the systematic error estimate. Some parts of the detector performance (including analysis performance) are already known from our E246 experience. Some parts are easy to estimate straightforwardly with only a small ambiguity without detailed Monte Carlo simulations. Thus, we set up our Monte Carlo study program to solve the problems most efficiently and reliably. In this report we present three major results of Monte Carlo studies which are decisive for the determination of the experimental sensitivity and the total systematic error, respectively:

(1) Active polarimeter analysis to estimate the statistical sensitivity of the experiment,
(2) Polarimeter alignment and the estimate of the systematic error from misalignments,
(3) Estimate of the systematic error due to contamination of $K_{\pi 2}$ decay in flight.

In addition to these Monte Carlo simulation results, we would like to report on the following points, in order to show the progress of E06 (TREK) preparations since the first PAC meeting.

- Since last year, we have started several **R&D studies for the detector elements** which we plan to upgrade, in order to check the basic performance of the new detector concept. Some results are reported to the FIFC meeting [1], and they are shown here only briefly.

- Regarding the **collaboration issues and funding** of the experiment, we think that we have to mention the current status, because there are several new situations to report. The policy for the **beam line** construction is also presented.

2 Statistical sensitivity estimate

2.1 Analysis policy for the polarimeter

The new active polarimeter enables a measurement of the energy E_{e^+} and angle θ_{e^+} of the muon decay positron. In the proposal we presented the possibility to analyze the decay event-by-event with a weight $\alpha(E_{e^+})/\cos\theta_{e^+}$. Here $\alpha(E_{e^+})$ is the energy dependent asymmetry function defined as $D(E)/C(E)$ at the e^+ energy E_{e^+}, where $C(E) = x^2(3-2x)$ and $D(E) = x^2(2x-1)$ are the isotropic and the asymmetric functions of the Michel spectrum, respectively ($x = 2E_{e^+}/mc^2$). This method is essentially different from the integral measurement and analysis which we applied in E246 [2], and will be able to provide the highest analytical sensitivity of $\delta P_T = 3.73/\sqrt{N}$[1]. However, in the course of recent considerations we came to the conclusion that we should be conservative in designing the polarimeter and we estimate the sensitivity for the safe analysis method, namely the integral method to use π^0 going to forward (fwd) or backward (bwd) directions in the CsI(Tl) calorimeter, and in which only bounds for E_{e^+} and θ_{e^+} are set. In the weighted analysis there would be additional systematics coming from the E_{e^+} and θ_{e^+} measurement, which have yet to be worked out. Application of the event-by-event technique should be possible at the time of the final data analysis.

In the proposal it was also suggested to involve the events with π^0 going to $left/right$ directions in addition to the fwd/bwd directions in the CsI(Tl) barrel. At the moment, however, we regard this scheme also as an optional one to increase the final sensitivity. There are several systematics to be checked before adopting this method. For example, the detection performance of spin precession under the 0.03 T transverse field has to be established, and also the field mapping accuracy has to be proved to make the analysis feasible.

Therefore, we present here primarily the Monte Carlo simulation of the safe but conservative estimate of the sensitivity only for the integral method for the conventional fwd/bwd π^0 regions.

2.2 π^0 fwd/bwd method and figure of merit for e^+ analysis

In the integral analysis we measure the so called T-odd positron asymmetry A_T which is defined as $A_T = \frac{1}{2}(A_{fwd} - A_{bwd})$ with the fwd and bwd asymmetries for the cases where π^0s are going in the forward (fwd) direction or backward (bwd) direction in the calorimeter. The asymmetry is calculated from the clock-wise and counter clock-wise positron emission rates as their relative difference (Eq. 27 of the proposal). The average value of P_T in the accepted kinematical region (hereafter we call it simply P_T instead of $< P_T >$) is then,

$$P_T = A_T/(\alpha < \cos\theta_T >), \tag{1}$$

where α and $< \cos\theta_t >$ are the analyzing power, and the angular attenuation factor due to the decay plane angular distribution in the finite decay kinematical region, respectively. In E06 (TREK) this analysis can be optimized by selecting only the sensitive regions in the energy spectrum and in the angular distribution by taking advantage of the active

[1] Hereafter, a standard deviation (one σ) error of P_T is denoted as δP_T.

polarimeter information. As seen from the muon decay Michel spectrum,

$$\frac{d^2\Gamma}{dxd\cos\theta_e} \propto x^2[3-2x+P_T(2x-1)\cos\theta_e] \tag{2}$$

the asymmetry is more sensitive to P_T in the larger E_{e^+} region and the larger $|\cos\theta_{e^+}|$ region, namely the analyzing power α is dependent on the lower bounds of the analyzed E_{e^+} and $|\cos\theta_{e^+}|$. Thus, we find the optimum condition. By taking into account the statistical significance which scales as $\sqrt{N_{e^+}}$ (N_{e^+} is the number of positron events in this analysis region), the figure of merit function defined as,

$$FoM = \alpha\sqrt{N_{e^+}} \sim A_T\sqrt{N_{e^+}} \tag{3}$$

was maximized in a Monte Carlo simulation[2] by varying the e^+ energy threshold (E_e^{th}) and the e^+ cone angle cut (θ_e^{th}). Fig.1 (a) shows a two dimensional (E_e^{th}, $\cos\theta_e^{th}$) contour plot of the FoM distribution. The best positions were obtained at E_e^{th} = 38 MeV and $\cos\theta_e^{th}$ =0.34 corresponding to $\theta_e^{th} = 70°$. The associated analyzing power is α =0.38. This value can be compared with the "nominal" asymmetry coefficient of 1/3 taking all the positron energy and also with the E246 analyzing power, $\alpha = 0.27$, with further reduction due to the smearing of the angular information in the passive polarimeter.

On the other hand, the average angular attenuation factor $< \cos\theta_T >$ was defined for the angle θ_T of the decay-plane normal vector relative to the ϕ axis in the polarimeter. Since $\cos\theta_T$ basically corresponds to the π^0 direction, the FoM function $< \cos\theta_{\pi^0} > \sqrt{N_{\pi^0}}$ (N_{π^0} is the number of accepted $K_{\mu 3}$ events) was again maximized by changing the cut position of the π^0 cone angle. The FoM dependence on θ_{π^0} is shown in Fig. 1 (b). The optimum position is $\cos\theta_{\pi^0}^{th} = 0.30$ and the average angular attenuation factor is $< \cos\theta_T >= 0.68$, similar to the value used in E246. Using the obtained α and $< \cos\theta_T >$, Eq.(1) leads to $P_T = A_T/0.258$.

2.3 Estimate of final statistical sensitivity

The number of $K_{\mu 3}$ events collected in the E06 experiment can be estimated as follows. The beam intensity at the K0.8 channel is assumed to be 2.1×10^6/s (which is less than 3×10^6/s in the proposal because of the change in the K1.1 upstream beam optics). Our beam request is accordingly 1.4×10^7s [1](See below). Therefore, the statistical sensitivity was calculated based on the total number of incident $K^+ = 3 \times 10^{13}$.

Regarding the detector acceptance, it was also evaluated in a Monte Carlo calculation. Requiring the standard selection conditions for $K_{\mu 3}$ events [2],

(1) $65 < M_{\gamma\gamma} < 185$ MeV/c^2,
(2) $3500 < M^2_{\mathrm{TOF}} < 18000$,
(3) μ^+ incident into the polarimeter,
(4) $P_\mu < 185$ MeV/c,
(5) $\theta_{\mu^+\pi^0} < 160°$, and
(6) (missing mass)$^2 > -15000$ MeV/c^2,

[2]A realistic condition was assumed for the muon stopping in the stopper as is described in the next Subsection 2.3.

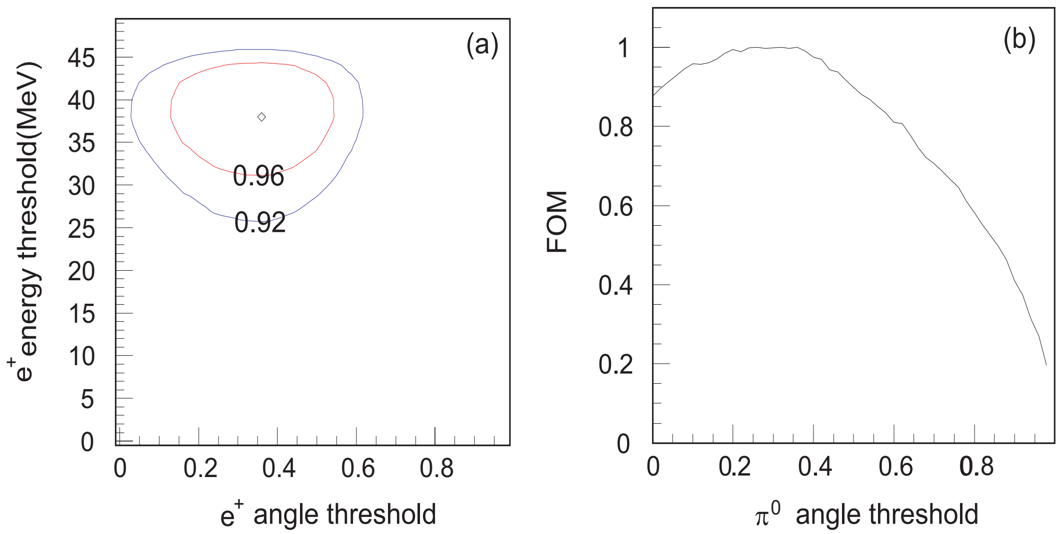

Figure 1: FUN distributions (a) two dimensional contour in terms of (E_e^{th}, θ_e^{th}) (b) dependence on π^0 cone angle cut. The maximum point of the FUN value is normalized to be 1.

the detector acceptance was determined to be $\Omega(K_{\mu3}) = 1.14 \times 10^{-2}$. Considering the $\sim$10 times larger acceptance in the active polarimeter, this acceptance is consistent with the actually observed acceptance in E246. The number of accepted $K_{\mu3}$ events, $Y(K_{\mu3})$, is then calculated as,

$$Y(K_{\mu3}) = 3 \times 10^{13} \cdot \epsilon_{stop} \cdot Br(K_{\mu3}) \cdot \Omega(K_{\mu3}) \tag{4}$$

where $\epsilon_{stop} \sim 0.3$ is the stopping probability of the K^+ beam in the target and $Br(K_{\mu3}) = 3.2\%$ is the $K_{\mu3}$ branching ratio. Note that $\Omega(K_{\mu3})$ does not includes the muon stopping efficiency in the stopper which is about 88%. Using these values, we obtain a total $Y(K_{\mu3})$ event number of 3.3×10^9.

In the present Monte Carlo simulation, total 10^8 $K_{\mu3}$ events were generated in front of the active polarimeter for $Y(K_{\mu3})$. Muons were stopped mainly in the central part the 31 stopper array. Hence, the muons stopped in the outermost 6 layers were discarded. (They are not very useful events anyway when the decay e^+s escape from the stopper by penetrating only a few layers of the stopper.) Positron asymmetries A_{fwd} and A_{bwd} were measured for positrons above E_{e^+} and θ_{e^+} and by selecting the relevant π^0 regions. P_T was then evaluated using the optimum α and $< \cos\theta_T >$ and a statistical accuracy of $\delta P_T = 6.9 \times 10^{-4}$ was obtained. (Actually a finite value of P_T was input in this simulation taking Im$\xi = -0.05$[3].) This leads to the relation of $\delta P_T = 6.9/\sqrt{N}$ where N is the number of $K_{\mu3}$ events in front of the stopper as Eq.(4). For the total number of events $Y(K_{\mu3}) = 3.3 \times 10^9$ in E06 we will obtain

$$\delta P_T = 6.9/\sqrt{33 \times 10^8} = 1.2 \times 10^{-4}. \tag{5}$$

[3]Imξ is the physics parameter of the transverse polarization P_T. See the proposal for the definition.

Table 1: Expected statistical sensitivity of E06 (TREK)

Parameter	E06 (TREK)	*c.f.* E246
K^+ intensity	2.1×10^6/s	1×10^5/s
Run time	1.4×10^7s	1.7×10^7s
Statistical error δP_T	1.2×10^{-4} (for fwd/bwd - π^0)	2.3×10^{-3}
	1.0×10^{-4} (for fwd/bwd+left/right - π^0)	–

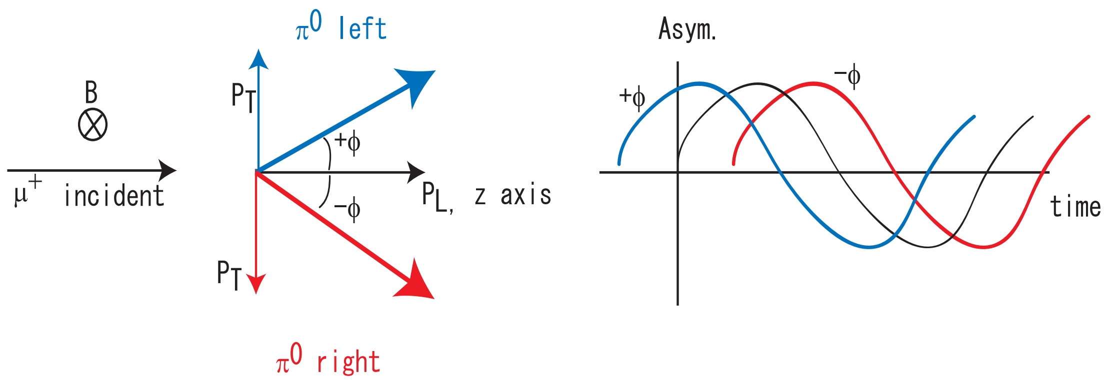

Figure 2: P_T extraction procedure in the π^0 *left/right* analysis. The existence of the finite P_T leads to phase shift of in-plane components in opposite direction.

Thus, a 19 times better statistical error of $\delta P_T = 1.2 \times 10^{-4}$ can be expected compared with the E246 statistical error of $\delta P_T = 2.3 \times 10^{-3}$.

2.4 Optional π^0 left/right analysis

It is worth mentioning the optional analysis of π^0 *left/right* events, to see roughly the gain in the sensitivity. The number of $K_{\mu 3}$ events will become approximately twice more and resulting in higher sensitivity. Since the π^0 *left/right* evens are subjected to a full P_T precession in the B field, the analysis should be time-differentially, and asymmetry fitting procedure to a precession pattern of e^+ is necessary for the P_T extraction.

An essential point for this analysis is the cancellation of the in-plane component P_L of the muon polarization by comparing events with the π^0 going *left* and *right*. Since the P_T direction can be flipped by selecting the π^0 direction, the existence of a finite P_T leads to a phase shift $\pm\phi$ of any P_T components in the opposite direction, as shown in Fig. 2. This phase shift can be extracted by comparing the e^+ time spectra of *left* and *right* π^0 events, because the P_L component is common for π^0 *left* and *right* events. Since the initial muon direction and hence the direction θ_0 of the in-plane component P_L is distributing in the $z-r$ plane, the dependence on θ_0 has to be taken into account in the analysis. Here two sets of the muon decay asymmetries can be considered: one is the asymmetry in the z-direction, A_z, and the other is the asymmetry in the radial direction, A_r. We are interested in the θ_0

difference of these asymmetries between the cases of π^0 going to $left$ direction L and $right$ direction R, especially their muon spin direction (θ_0) dependence. Namely,

$$\tilde{A}_z(\theta_0) = \frac{A_z^L(\theta_0) - A_z^R(\theta_0)}{2} \tag{6}$$

$$\tilde{A}_r(\theta_0) = \frac{A_r^L(\theta_0) - A_r^R(\theta_0)}{2}, \tag{7}$$

Here, θ_0 is determined event-by-event from the decay kinematics condition with $K_{\mu 3}$ form factors. For details see the explanation in Appendix A. Fig. 3 (a) shows the simulated A_z^L and A_z^R time distributions at θ_0=0 bin. If the P_T component exists, an oscillation pattern appears in the subtracted spectrum $\tilde{A}_z(\theta_0)$ as shown in Fig. 3 (b). Here, in the Monte Carlo simulation we assumed an exaggerated value of P_T corresponding to Imξ=-0.50. Hence, P_T can be extracted from the oscillation pattern of $\tilde{A}_z(\theta_0)$ as well as $\tilde{A}_r(\theta_0)$. They can be written as,

$$\begin{aligned} \tilde{A}_z(\theta_0) &= \epsilon \cdot \cos(\omega t + \beta) && (8) \\ \tilde{A}_r(\theta_0) &= \epsilon \cdot \sin(\omega t + \beta). && (9) \end{aligned}$$

where ϵ and β are fitting parameters corresponding to the amplitude from the P_T component and the phase rotation at each θ_0, respectively. The amplitude ϵ scales with P_T and the phase β should be a function of θ_0 for both A_z and A_r. The parameter ϵ (namely P_T) can be deduced with the highest sensitivity in this way in the presence of a finite θ_0 range. Fig. 3 (c),(d) shows the fitting results of the simulation data for the ϵ and β values. The statistical error of P_T was estimated by making an error weighted average of ϵ over θ_0. By converting the Monte Carlo event number to the total E06 event number, we obtain a sensitivity of

$$\delta P_T = 1.6 \times 10^{-4}, \tag{10}$$

which is a comparable to the level from the π^0 fwd/bwd analysis, Since the π^0 $left/right$ and fwd/bwd events are cumulative data and the analyses are performed independently, it is possible to calculate the combined P_T sensitivity as

$$\delta P_T = 1.0 \times 10^{-4}. \tag{11}$$

It is stressed once again that a careful check of the systematic error due to admixture of the in-plane component must be carried out.

2.5 Update of run time request

In the proposal we requested a beam time of net 1.0×10^7 s for the main measurement. This request was based on the estimate of the K^+ beam intensity at K1.1-BR, $3{\times}10^6$/s. The beam optics of K1.1-BR were designed at that time according to the upstream layout of the K1.1 beam line [3]. However, in the course of the actual detailed design of the front-end part K1.1 as the counter part of K1.8, the J-PARC facility group decided to put the first bending magnet B1 at 2 m from the target (*i.e.* 0.8 m further than in the original design (See Section 4 of Ref. [1]). The consequence was the reduction of the channel acceptance from 6.0-6.5 msr($\Delta p/p$%) to 4.5 msr($\Delta p/p$%). The expected K^+ intensity is now $\sim 2.1 \times 10^6$/s [4], although the beam quality such as the K/π ratio won't be changed. Accordingly, the net run time is modified and it is now $1.4{\times}10^7$s.

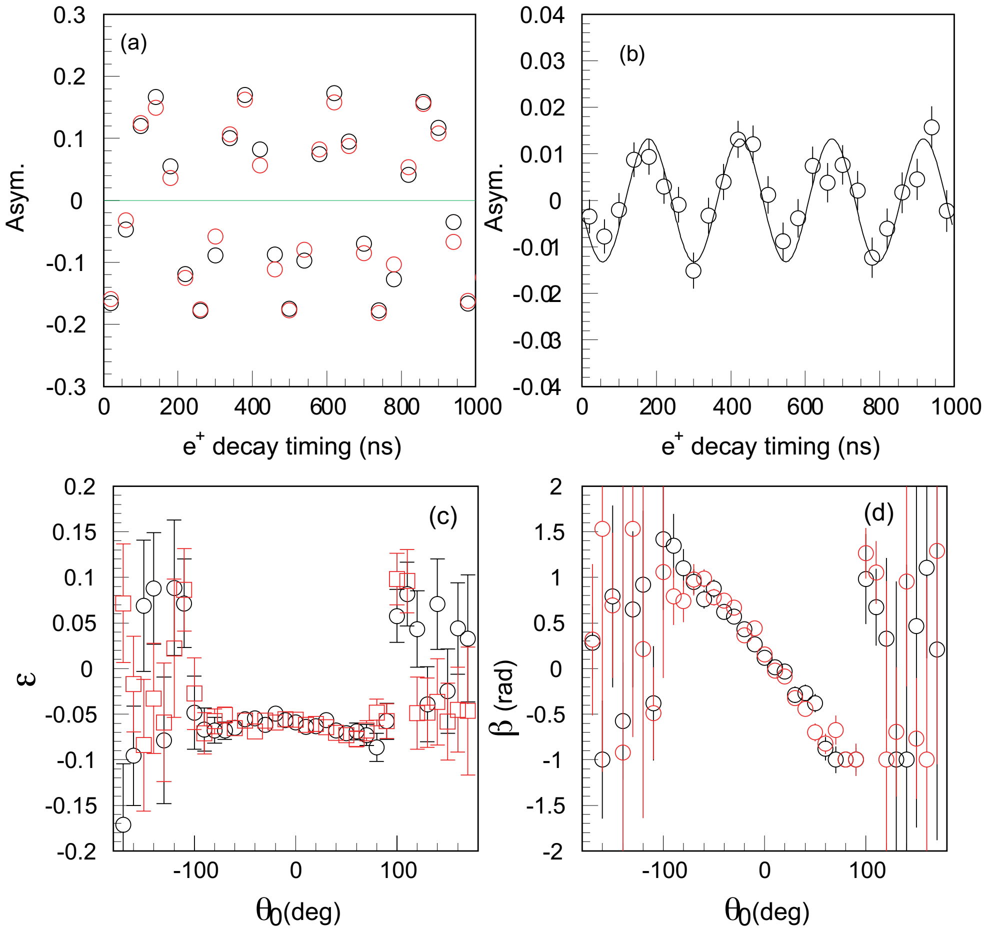

Figure 3: (a) A_z^L (red) and A_z^R (black) distribution for $\theta_0 = 0$ bin and (b) subtracted spectrum, namely $\tilde{A}_z(\theta_0 = 0)$. P_T value corresponding to Imξ=-0.50 was assumed here. Although strong contribution from in-plane component is observed in A_z^L and A_z^R, the pure P_T component is extracted by their subtraction. Fitting results of the π^0 $left/right$ analysis for (c) ϵ and (d) β. In (c) and (d), red and black circles are from $\tilde{A}_z$ and $\tilde{A}_r$, respectively. The statical error of P_T is estimated by making error weighted average of ϵ.

3 Systematic error analysis

3.1 Possible sources of systematic errors

The possible sources of systematic errors are listed in Table 28 of the proposal along with their suppression goals. The shifts of the decay plane distribution due to unbalanced detector response parameterized with two rotation angles of $< \theta_r >$ and $< \theta_z >$ were treated as systematic errors in E246 because their sizes were smaller than the final statistical error. In E06 (TREK), with the suppression of the systematic errors by a factor of 10, it is inevitable to make a correction for these rotations. If necessary one applies an artificial symmetrization on the distribution of θ_r and θ_z by discarding some, otherwise good, events. The influence of the finite shifts of the mean value of the distributions on P_T are $\delta P_T \sim 0.5 < \theta_r >, \sim 0.5 < \theta_z >$. Therefore, the statistical uncertainty of the corrections scales as $\sigma_\theta/\sqrt{N}$ which should be smaller than δP_T^{stat} even for θ_z for which the π^0 fwd/bwd cancellation does not work.

New systematics associated with the threshold setting for E_{e^+} and $\cos\theta_{e^+}$ is essentially π^0 fwd/bwd cancelling up to a potential slight difference in the muon stopping distribution in the stopper. If this is significant one may symmetrize the fwd/bwd stopping distribution by discarding a small faction of, otherwise good, events. Hence, we regard this systematic error as controllable one. Note that the largest systematic error in E246, the effect of multiple scattering on the muon stopping position, is not relevant any more in E06 where the active polarimeter can locate the muon stopping point with high precision.

The major systematic errors in E06, therefore, arise from the detector element misalignment, especially the misalignments of the active polarimeter and the muon field distribution, which can both be studied in MC simulations and the details are shown below. Another conceivable source of the systematic error is the contamination of $K_{\pi 2}$ decay-in-flight background. The Monte Carlo study of this problem is also shown in Subsection 3.9.

3.2 Polarimeter alignment

3.2.1 General alignment method

As was discussed in the proposal in considerable detail, the alignments of the tracking system and the CsI(Tl) calorimeter system relative to the reference system of the spectrometer will be performed using a set of calibration collimators for the former and $K_{\pi 2}$ events for the latter. Although careful designs are required for both, we regard the calibration procedure to be rather straightforward; the performance of the calibration can be easily checked with simulations. They are all fwd/bwd cancelling and thus controllable. On the contrary, the effect of polarimeter misalignments, which are direct systematics affecting the positron asymmetry, A_T, are complicated with the entanglement of several factors including the muon field. Moreover, one of the misalignments, the rotation of the muon field around the z-axis δ_z, is a systematic which cannot be canceled out in the normal π^0 $fwd/bwad$ subtraction scheme. In the following we present the alignment method of the polarimeter, which we regard as the most important in this experiment.

3.2.2 Misalignments and positron asymmetry

The basic idea of the polarimeter alignment was also given in the proposal. Here, we would like to proceed with that argument further and to present a method to extract the misalignments and to determine P_T at the same time. A Monte Carlo calculation (The details are described in Appendix A) verifies the validity of this method.

As was discussed in the proposal, the misalignments of the polarimeter are characterized by four parameters (See Fig. 32 of the proposal) – 1) global rotation of the active stopper around the r-axis: ϵ_r, 2) global rotation around the z-axis: ϵ_z, 3) global rotation of the muon field distribution around the r-axis: δ_r and 4) global rotation around the r-axis: δ_z. They are only responsible for spurious A_T; parallel displacements should not play a role as long as the active stopper covers the whole muon stopping region because of the parallel-shift symmetric structure. The rotation about the y-axis should not have any effect since it brings about only a rotation around the azimuthal axis.

In the following we show how to determine these four rotation misalignments. When these four misalignments exist a precession pattern with a small amplitude appears in the e^+ $left/right$ asymmetry. For the typical two cases of in-plane polarization of longitudinal polarization P_l and radial polarization P_r. The asymmetries can be written as

$$A(P_l) = \alpha_0\{(\epsilon_r - \delta_r)\cos\omega t + (\epsilon_z - \delta_z)\sin\omega t + \delta_r\} \tag{12}$$

$$A(P_r) = \alpha_0\{(\epsilon_r - \delta_r)\sin\omega t - (\epsilon_z - \delta_z)\cos\omega t - \delta_z\} \tag{13}$$

Here, ω is the muon spin precession angular velocity, and α_0 is the asymmetry coefficient for these rotations[4]. More generally, the asymmetry, A, can be expressed for arbitrary initial muon spin phases θ_0 in the median plane (as shown in Fig. 4) as:

$$\begin{aligned} A(\omega t, \theta_0) = {} & \alpha_0\{(\epsilon_r - \delta_r)\cos(\omega t - \theta_0) + (\epsilon_z - \delta_z)\sin(\omega t - \theta_0) \\ & + \delta_r\cos\theta_0 - \delta_z\sin\theta_0\} + \gamma \end{aligned} \tag{14}$$

Here we add an additional offset term γ due to a possible asymmetric muon stopping distribution in the stopper or some unknown polarimeter defects such as a chamber inefficiency. Rotation of the magnetic field generates the constant $\delta_r\cos\theta_0 - \delta_z\sin\theta_0$ term which mimics the actual T-violation effect. In the proposal we showed a possibility to use $K_{\mu2}$ and μ^+ from decay-in-flight of π^+ in the $K_{\pi2}$ decay ($K_{\pi2}$-dif) to produce P_l and P_r, respectively. Here, we present another method to use $K_{\mu3}$ events of the main data. We now regard this to be more promising, since it does not require special runs with modified experimental conditions, and it is also not limited by statistical accuracy as in the case of $K_{\pi2}$-dif.

3.2.3 Alignment analysis in terms of muon spin direction

When we apply this method of analyzing the θ_0 dependence, the $K_{\mu3}$ events can be used fully. For each $K_{\mu3}$ event, θ_0 can be calculated from the decay kinematics as explained in Appendix A.5. In order to simplify the analysis, the time integrated asymmetry was introduced as follows.

$$\begin{aligned} \bar{A}(\theta_0) = {} & \int[\alpha_0\{(\epsilon_r - \delta_r)\cos(\omega t - \theta_0) + (\epsilon_z - \delta_z)\sin(\omega t - \theta_0)]dt \\ & + \delta_r\cos\theta_0 - \delta_z\sin\theta_0\} + \gamma, \end{aligned} \tag{15}$$

[4] These equations are the same as Eq.(30) of the proposal in which α_0 was omitted for simplicity.

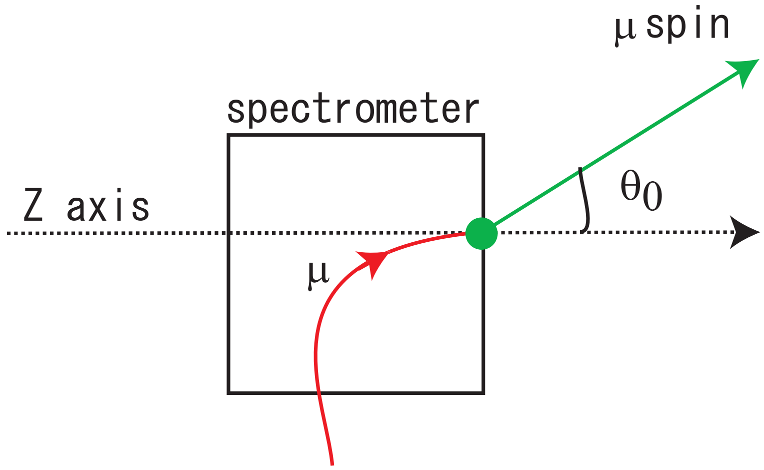

Figure 4: Definition of θ_0 angle. The original muon spin direction was obtained from the kinematics of $K_{\mu 3}$ decay products with a form of [1]. The θ_0 value of each $K_{\mu 3}$ decay at the muon stopping position in the polarimeter is determined by taking into account the muon spin rotation by the spectrometer field.

The oscillation terms are averaged out by the time integration and become less harmful compared to the non-oscillating terms. The contribution due to imperfect cancellation of the oscillation term (η) can be described as a function of θ_0 and the time integrated asymmetry is thus rewritten as,

$$\bar{A}(\theta_0) = \alpha_0\{\delta_r \mathrm{cos}\theta_0 - \delta_z \mathrm{sin}\theta_0 + \eta(\theta_0)\} + \gamma, \qquad \eta << \delta \tag{16}$$

which is a rather simple form compared with Eq.(15). The ϵ terms are removed by the time integration. Here it should be noted that the spurious asymmetry from the misalignments depends only on θ_0.

In order to extract the misalignment parameters δ_r and δ_z in the presence of a real P_T, we now calculate two asymmetries A_{sum} and A_{sub} as functions of θ_0 such as the sum and difference of A_{fwd} and A_{bwd} with the asymmetries at the forward and backward pions, respectively. This leads to

$$\begin{aligned} A_{sum}(\theta_0) &= (\bar{A}_{fwd}(\theta_0) + \bar{A}_{bwd}(\theta_0)/2 = \alpha_0\{\delta_r \mathrm{cos}\theta_0 - \delta_z \mathrm{sin}\theta_0 + \eta(\theta_0)\} + \gamma && (17) \\ A_{sub}(\theta_0) &= (\bar{A}_{fwd}(\theta_0) - \bar{A}_{bwd}(\theta_0))/2 = F(P_T, \theta_0). && (18) \end{aligned}$$

Here, $F(P_T, \theta_0)$ is the A_T asymmetry function only from P_T origin and it does not involve any misalignment effect. Thus, we have no effects of P_T in A_{sum} and no effects of misalignments in A_{sub}, enabling the determination of $F(P_T, \theta_0)$ unaffected by the misalignments. From $F(P_T, \theta_0)$ (which is nearly an even function of θ_0), P_T can be deduced, Further, δ_z and δ_r can also be individually determined by fitting A_{sum} with $\cos\theta_0$ and $\sin\theta_0$. The behaviours are shown in Fig. 5 (a) for A_{sub} and Fig. 5 (b) for A_{sum} for Monte Carlo simulation data which we describe next,

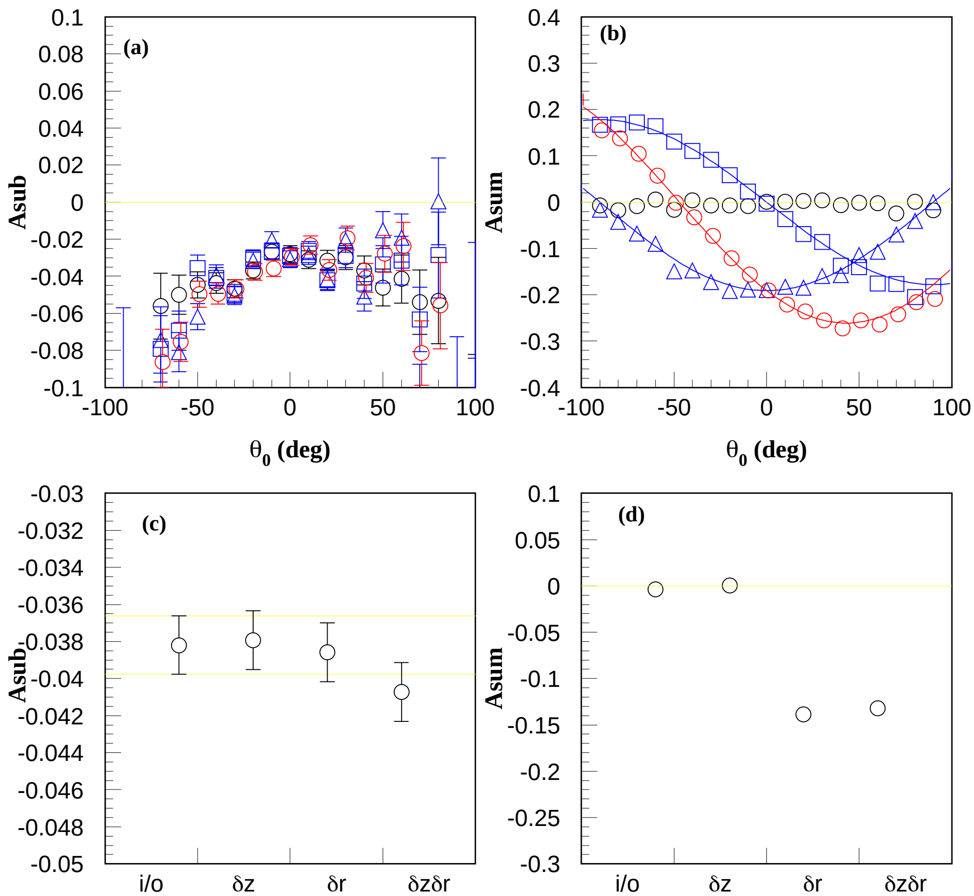

Figure 5: (a),(b) Muon polarization distribution derived from A_{sub} and A_{sum} with various conditions and (c),(d) their error weighted averages, black (ID=1): Im(ξ)=0.05, $\delta = 0$, blue square (ID=2): Im(ξ)=0.05, $\delta_z = 5°$, blue triangle (ID=3): Im(ξ)=0.05, $\delta_r = 5°$, red (ID=4): Im(ξ)=0.05, $\delta_z = 5°$, $\delta_r = 5°$. The polarization was converted from the e^+ asymmetry corrected for the analyzing power α_0.

3.2.4 Monte Carlo simulation

How this analysis scheme works was checked with a Monte Carlo simulation, whose details are described in Appendix A. Briefly it is explained as follows. Assuming the existence of both Imξ and δ (with exaggerated values) at the same time, the above A_{sum} and A_{sub} were calculated. Fig. 5 (a),(b) shows the A_{sub} and A_{sum} distributions, respectively, corrected for the analyzing power of the polarimeter as, black circle: Im(ξ)=0.05, $\delta = 0$, blue square: Im(ξ)=0.05, $\delta_z = 5^\circ$, blue triangle: Im(ξ)=0.05, $\delta_r = 5^\circ$, and red circle: Im(ξ)=0.05, $\delta_z = 5^\circ$, $\delta_r = 5^\circ$. Although they were obtained with various combinations of Imξ and δ, in any cases, we see no effects of misalignments in A_{sub} as was expected. Also we see obviously the behaviors of Eq.(17) in A_{sum}. The A^{av}_{sub} and A^{av}_{sum} values with the simultaneous existence of Imξ and δ were compared with those with single Imξ or δ cases, as shown in Fig. 5 (c),(d). They are consistent within errors, indicating the reproducibility of δ_r and δ_z in the admixed existence and the validity of the $A_{sub}(A_{sum})$ scheme.

For the planned run time we expect (by scaling this result statistically) an alignment accuracy of $\Delta\delta_r \sim \Delta\delta_z \sim 3\times10^{-4}$ from the analysis of A_{sum} shape, as well as a P_T accuracy of 1.2×10^{-4} from A_{sub}, which is just the same value we gave in Section 2 (Table 1) providing the second confirmation of the sensitivity estimate.

3.2.5 Systematic error due to the misalignment

In order to estimate the systematic error associated with the analysis the following consideration is valid. In this simulation study, we tested a case with Im$\xi = 0$ but with an exaggerated assumption of $\delta_z = 5^\circ$ and $\delta_r = 5^\circ$ with 100 million events. The obtained averaged A_{sub} value was $A^{av}_{sub} = (2 \pm 7) \times 10^{-4}$ which was consistent with zero. However, this value could be also regarded as the size of the ambiguity for A^{av}_{sub}. Taking into account that the actual field rotation is expected to be at the level of ~1mrad and that the current large error of A^{av}_{sub} is due to statistical accuracy, a much smaller value is anticipated in the real run. Furthermore, taking into account the cancellation power of the A_{sub} analysis for the spurious e^+ $left/right$ asymmetry, the systematic error due to this analysis is estimated to be smaller than $\delta P_T < 10^{-4}$.

Also, the misalignment measurement by the A_{sum} analysis can assure the reliability of the δ determination by checking the consistency with the results from $K_{\mu2}$ and $K_{\pi2}$-dif data (See below). Therefore, from both (1) cancellation of the misalignment effects by A_{sub} and (2) understanding of the misalignments by A_{sum}, we can reliably control the systematic error from the field misalignment to a negligible level.

Other potential sources such as the misalignment of tracking elements are regarded to be rather harmless since the correction based on the alignment calibration can be done accurately enough. Each correction is applied with an uncertainty of less than 10% of the correction values and the total systematic error by adding all the items can be made as small as 10^{-4}.

3.2.6 Redundant alignments using $K_{\mu2}$ and $K_{\pi2}$ events

Since measurement of the misalignments is essential, a redundant measurement other than $K_{\mu3}$ events is highly desirable. In order to do that, we will utilize the longitudinal polarization of $K_{\mu2}$ (events with $\theta_0 \sim 0$) and the muon polarization from decay-in-flight π^+ of $K_{\pi2}$ decays (events with $\theta_0 \sim -\pi/2$ or $\sim \pi/2$) (See the proposal).

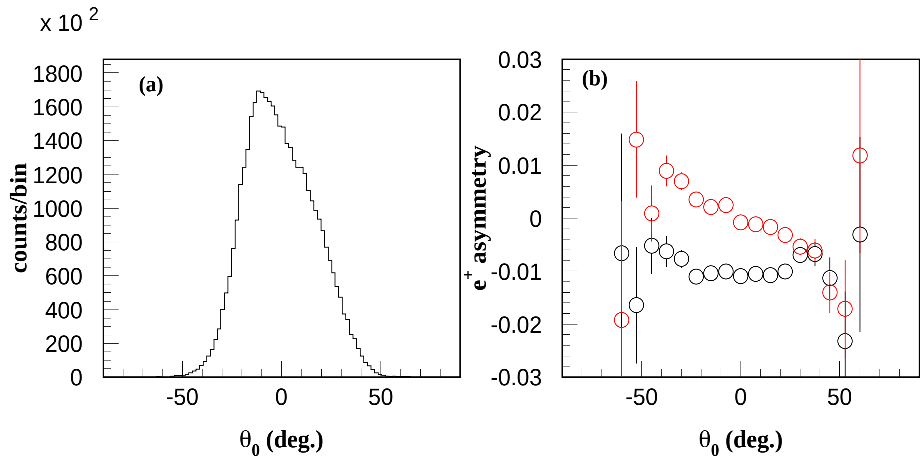

Figure 6: (a) θ_0 distribution of the $K_{\mu 2}$ events and (b) their time integrated asymmetry of as a function of θ_0 for the case of the finite δ_z (red circles) and δ_r (black circles) terms. The $K_{\mu 2}$ events are concentrated around $\theta_0 = 0$ and are sensitive to δ_r. In this simulation the magnetic field of the toroidal spectrometer was raised to 1.35 T from 0.9 T of the normal run.

The former and the latter are sensitive to δ_r and δ_z, respectively. The transverse decay of a π^0 in the CM system with a muon emitted in the gap median plate produces a polarization component of the stopped muon in the radial direction. Radial and longitudinal components of $K_{\mu 2}$ muon polarization are also available to determine the misalignments. The polarization calibration should be performed using both in-flight $K_{\pi 2}$ muons and $K_{\mu 2}$ muons independently and compared with the results obtained using $K_{\mu 3}$ events. Since it is possible to determine θ_0 for both $K_{\mu 2}$ and $K_{\pi 2}$ decays, the time integrated e^+ asymmetry can be obtained as a function of θ_0. Fig. 6 (a),(b) show the θ_0 distribution of the simulated $K_{\mu 2}$ events and their $left/right$ asymmetries, respectively. The sin and cos oscillation patterns in the asymmetries corresponding to δ_z and δ_r were observed in (b), which should be consistent with the $K_{\mu 3}$ results. One day of the special trigger run with an increased spectrometer field should provide enough statistics. Thus, the systematic check by this measurement of misalignments using $K_{\mu 2}$ and $K_{\pi 2}$ decays will play an important role to strengthen the reliability of the alignments.

3.3 $K_{\pi 2}$ decay-in-flight background

3.3.1 New tracking system

Along with the polarimeter alignment, the suppression of $K_{\pi 2}$ decay-in-flight background contamination is essential to achieve the total systematic error of the size of $\preceq 10^{-4}$. Since these events present a background that has a transverse polarization component, they should be sufficiently suppressed. In E246 in which we had only the minimum charged-particle

Table 2: Comparison of the tracking performances for the E246 and E06

	ΔP_{gap}	ΔP_{loss}	ΔP_{cor}	ΔK_{diff}	A_{diff}	$K_{\pi 2}$-dif BG
E246	1.0 MeV/c	2.5 MeV/c	2.5 MeV/c	20 mm	$\sim 2.0°$	2.4%
E06 (TREK)	0.5 MeV/c	0.85 MeV/c	1.0 MeV/c	0.6 mm	0.3°	0.2%

tracking system, a few % admixture in the $K_{\mu 3}$ data was unavoidable. In E06 (TREK) we will improve the tracking system. The main feature is the addition of C0. For sufficient identification and suppression of $K_{\pi 2}$ events it is required to build a cylindrical tracking chamber ("C0") with a radius of several cm surrounding the target and with a spatial resolution of <0.1 mm. Four-point tracking including C0 should significantly enhance the achievable resolution for track momentum and origin at the target. A new planar tracking element (again named "C1") increases redundancy with <0.1 mm resolution to cover each of the 12 gaps at the outer surface of the CsI(Tl) calorimeter. The new tracking elements C0 and C1 will be based on GEM technology (Gas Electron Multiplier) which has recently become available. A cylindrical geometry with curved GEM foils are also possible. GEM detectors are radiation-hard and well suited to be operated in high-rate environments.

3.3.2 Expected performance of background rejection

The tracking performance was checked by a Monte Carlo simulation using $K_{\mu 3}$ events. Four elements, C0, C2, C3, and C4 were used with their expected performance. The radius of 5 cm was assumed here for the C0 readout layer. C1 was not included, which ensures that the obtained result is a conservative estimate of the system performance. Fig. 7 shows distributions of (a) χ^2, (b) difference of true and measured momentum, (c) distance between the trajectory and the K^+ decay position (K_{diff}), and (d) difference of true and measured μ^+ angle at the decay position (A_{diff}). The P_{gap}, K_{diff}, and A_{diff} resolutions are obtained to be 0.5 MeV/c, 0.6 mm, and 0.3°, respectively. Then, the original momentum (momentum at birth), P_{cor}, is calculated from P_{gap} by correcting for the momentum loss P_{loss} in the target as,

$$P_{cor} = P_{gap} + P_{loss}. \tag{19}$$

The path length in the target obtained from the charged particle trajectory and K^+ decay positron is used for the P_{loss} correction. The P_{cor} resolution is estimated to be 1.0 MeV/c which is dominated by the P_{loss} fluctuation of ΔP_{loss} = 0.85 MeV/c. The improvements are as summarized in Table 2.

The ability to suppress background events of $K_{\pi 2}$-dif is also obvious. Basically π^+-dif beyond C0 can be easily identified by χ^2 of tracking and we can reliably reject those events. However, for π^+-dif events between the target and C0 the χ^2 cut does not work anymore, and only the reliable information for the rejection is the transverse difference of a fit trajectory and a decay vertex in the target, K_{diff}. Fig. 7(c) shows the K_{diff} distribution for $K_{\mu 3}$ (black) and $K_{\pi 2}$-dif (red). The $K_{\mu 3}$ events are selected by requiring $K_{diff} < 1.8$ mm and the $K_{\pi 2}$ fraction in the $K_{\mu 3}$ sample is estimated to be 0.2% which is sufficiently small to achieve a systematic error much less than 10^{-4} in δP_T, because the further cancellation by gap L/R symmetry should be nearly a factor of 10^2.

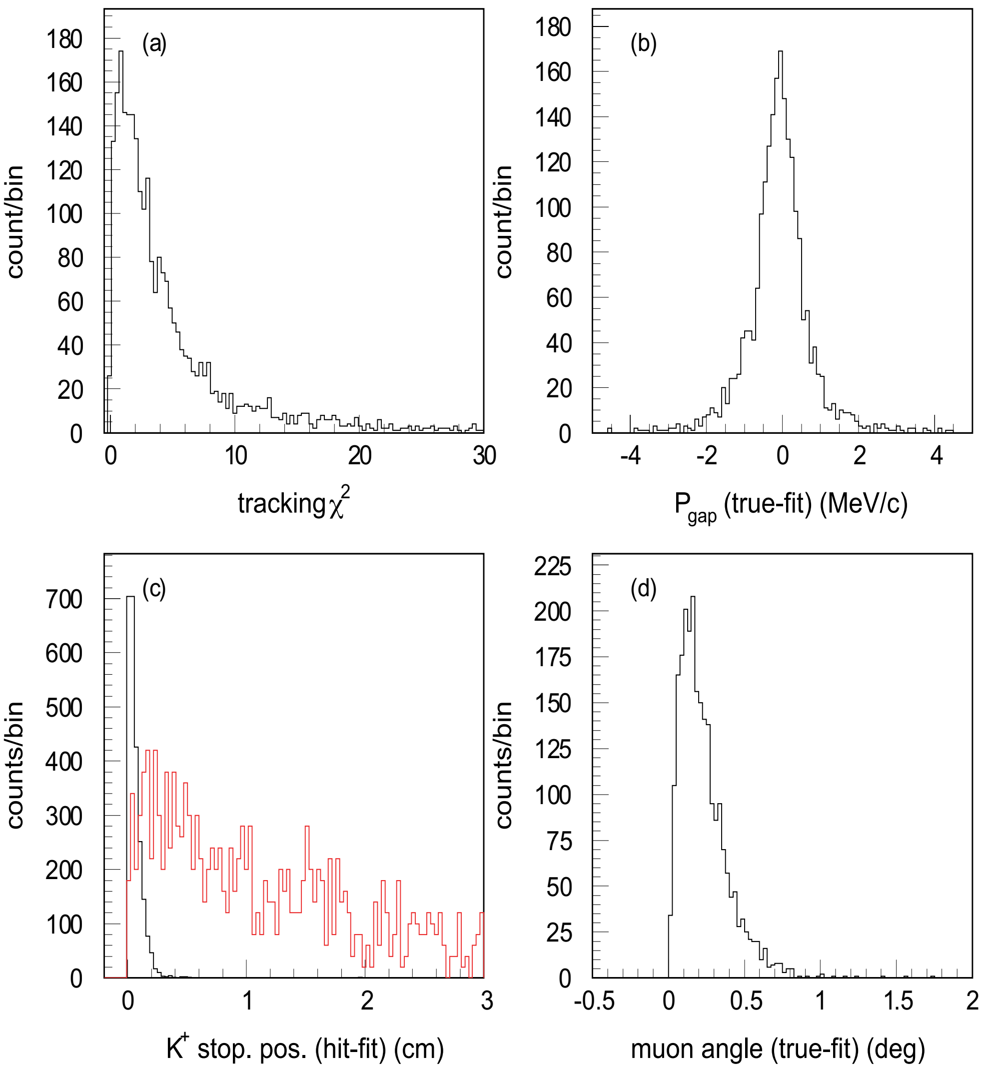

Figure 7: Tracking performance: (a) χ^2, (b) difference between true and measured momentum, (c) distance between the trajectory and the K^+ decay position (K_{diff}), and (d) difference between true and measured μ^+ angle. In-flight $K_{\pi 2}$ events are shown in (c) as red histogram.

Table 3: Expectation of the systematic errors in E06

Source	$\delta P_T^{syst}(10^{-4})$	Method
Polarimeter misalignment ($\delta_z, \delta_r, \epsilon_z$ and ϵ_r)	< 1	confirmed by MC simulation
$K_{\pi 2}$-dif background	$\ll 1$	confirmed by MC simulation
Decay plane rotations (θ_z and θ_r)	< 1	correction and data symmetrization
Positron analysis (E_{e^+} and θ_{e^+})	< 1	fwd/bwd cancellation and fwd/bwd symmetrization *etc.*
Total	$\delta P_T^{syst} \preceq 10^{-4}$	quadratic sum

3.4 Summary of systematic errors

As the consequence of the Monte Carlo studies reported in this section, the systematic error table of the proposal (Table 28: "Expectation of systematic error suppression") is revised to Table 3.

4 Progress of detector R&D for upgraded elements

4.1 Confirmation of basic performance

Since the stage-1 approval of E06 (TREK) last summer we have begun several R&Ds for the upgraded detector elements. The main purpose of these studies was to check the very basic performance of the proposed new schemes before proceeding to detailed design of those elements, and the studies were all small test experiments. Hence, detailed parameter determinations were not intended. Because we do not yet have any dedicated budget for such studies, they were mostly done with the kind support of constituent institutions of the group. For the active polarimeter, CsI(Tl) readout, fiber target, new GEM chambers we have obtained some very basic data which enables us to go further in the detector design. Details have recently been reported to FIFC [1] and they will not be repeated here. Only a short summary is presented below.

4.2 R&D/ test measurements and their results

Test measurements were performed at different places by several constituent groups of the collaboration to check the most urgent detector parts.

4.2.1 Active polarimeter

The most essential part of the active polarimeter is the muon stopper. The stopper has to preserve the muon spin polarization after stopping. Although an external field of 0.03 T is applied to suppress the spin relaxation, it is definitely necessary to test the muon spin behaviour for candidate stopper materials. We performed μSR measurements using a muon beam at TRIUMF by obtaining a dedicated beam time (E1120) of 72 hours. We confirmed that the candidate metals and alloys of Al and Mg show good enough characteristics in the initial polarization and spin relaxation with a 0.03 T field, also justifying this field strength.

4.2.2 CsI(Tl) readout

We are going to replace the current PIN diodes with APD diodes for the CsI(Tl) readout. This is a necessary upgrade to increase the rate capability of the colorimeter. There is, however, no case yet where a large Cs(Tl) crystal is read by an APD, although CMS has applied it to PWO for a 10 to 100 GeV range. It was urgent to check the matching and electron yield. A spare CsI(Tl) module of E246 was read by a Hamamatsu APD (S8148) of 5×5 mm^2 or 10×10 mm^2 area. For cosmic ray energy deposits of 15 to 20 MeV, a high enough electron yield of 47,000 e/MeV was observed. A good timing resolution of 3 ns and short pulse shape of 1.5 μs could be confirmed.

4.2.3 Fiber target

The current baseline design of the active fiber target is a bundle of scintillating fibers with a size of 2.5×2.5 mm^2 and 20-cm length. This size is 1/2 size of the E246 target fiber. Moreover, we will use SiPM/MPPCs for readout. It was urgent to check the bottom-line condition of this scheme by using a fiber sample of the current size. Two cases were tested; one was the use of a 3×3 mm^2 SiPM (MAPD from Dubna-Micron Co.) and the other was the use of a Hamamatsu 1×1 mm^2 MPPC (S10362-11) with one end of the scintillator stick tapered to 1×1 mm^2 cross section. For the former an photo-electron yield of 35 was observed while for the latter it was about 20. These data facilitated the further design to use an optical clear fiber extension.

4.2.4 MPPC radiation hardness test

As a joint project with several other experiments, radiation hardness tests of MPPC (S10362-11-50C) were performed using a direct proton beam at the Research Center for Nuclear Physics (RCNP). Since our target assembly will be exposed to the beam halo, this study was important to design the target assembly. Assuming a BeO beam degrader in front of the target the fluxes of K^+, π^+, μ^+, e^+ and neutrons were evaluated In a GEANT4 simulation. In the irradiation an increase of leakage current proportional to the total irradiation dose was observed. This total dose roughly corresponds to several months of the E06 run. The effect of the increased noise rate due to the leakage current is now being investigated.

4.2.5 C0 and C1 GEM chambers

In E06 we are going to add two new chambers, C0 and C1, to improve the tracking performance. C0 will be a cylindrical GEM chamber surrounding the target, and C1 will be a planer GEM chamber covering the muon hole. The GEM laboratory of MIT will produce these new chambers. An array of three MIT prototype triple GEM chambers made with Tech-Etch GEM foils has been beam-tested at FNAL. Stable operation was demonstrated. From the observed correlation distribution a spatial resolution of 90 μm could be concluded. Also a rate capability of at least 5 kHz/mm^2 (There was a large ambiguity from 5 kHz to 50 kHz due to the inaccurate beam density estimate.) was confirmed. This performance is also good enough for C0.

4.2.6 TOSCA magnetic field calculations

For the design of the muon field magnet, there are three major choices which have to be settled at the beginning. 1) Field direction should be parallel or anti-parallel to the superconducting toroidal magnet? 2) The current shim plate system should be kept or removed? 3) Is the decoupling of the SC toroidal fringing field by means of an end-plate necessary? In order to answer these questions, a TOSCA/OPERA 3D calculation was done. We decided to adopt 1) a parallel field configuration (as opposed to the proposal), 2) to keep the shim plates, and 3) not to put any field decoupling end plates. The unbalanced force acting on the SC coils in the cryostat is now being investigated.

Table 4: Summary of R&D for E06 (TREK) in this one year

Element	R&D item	Group/Place	Results	Conclusion
Polarimeter	Stopper μSR	Canada,Japan /TRIUMF	Relaxation rate (λ^{TF}, λ^{LF})	Al, Mg alloys
CsI(Tl)	APD readout	INR/INR	C.R. electron yield E-width, t-resol.	APD readout is O.K.
Target	MPPC readout	INR,KEK /INR,KEK	*p.e.* yield	2.5×2.5 mm^2 O.K. MPPC readout O.K.
Target-MPPC	Rad. hardness	Japan/RCNP	Leakage current	being investigated
C0 and C1	GEM chamber	MIT/FNAL	Stable operation x-resol., rate cap.	C0, C1 of GEM
μ^+ magnet	3D calculation	Japan/KEK	Field direction etc.	No problem in design

5 Status of collaboration and funding

5.1 Current status of collaboration

The current collaboration members are listed in Table 5 not including students. A change since the last PAC meeting (at the time of proposal) is the participation of the INR (Russia) group with some members who have experience in E246. We have also started a collaboration with Vietnam. At the present stage of approval we are still a relatively small group, but of course we will make an effort further to attract additional collaborators. Noted that the foreign teams from Canada, US, and Russia are playing very active and important roles. The university faculty members in Canada and the US will be able to attract graduate students in the future – once the beamline construction schedule is established.

5.2 International cooperation

In the proposal we presented the framework of the international cooperation for E06 (TREK). This scheme has recently been confirmed in the collaboration meeting held in February 2007. Each constituent country is responsible for some parts of the detector elements.

- North American universities led by Prof. W. Anderson is responsible for the design and production of the fiber target. The engineering design and construction will be done in the Detector Development Facility at TRIUMF under the supervision of R. Henderson. This same group was similarly responsible for the E246 target.

Table 5: E06 (TREK) experimental group

Country	Institution	Member
Canada	Univ of Saskatchewan (US)	C.Rangacharyulu[2], R.E.Pywell, M.Bradley
	Univ of British Columbia /TRIUMF	M.Hasinoff, J.Doornbos, D.Gill, R.Henderson, P.Gumplinger
	U. Montreal (UM)	P.Depommier
U.S.A.	MIT	M.Kohl. R.Milner, B.Surrow, D.Hasell, J.Kelsey, M.Plesko, F.Simon
	Iowa State Univ.(ISU)	W.Anderson
	Univ of South Carolina (USC)	S.Strauch, C.Djalali
Russia	INR (Moscow)	A.Ivashkin[3], A.Sadovsky, A.Kurepin
Vietnam	Nat.Sci.Univ in HCNC	D.P.Nguyen, C.V.Tao, T.Hoang
Japan	KEK	J.Imazato[1], G.Y.Lim, Y.Igarashi, H.Nakayama, S.Sawada, H.Shimizu
	Osaka U.	S.Shimizu[4], K.Horie
	Kyoto U.	T.Tsunemi
	Tohoku U.	H.Yamazaki
	Nat.Defnse Acad.	T.Matsumura

1) Spokesperson, 2) Foreign co-spokesperson, 3) Leader of Russian team, 4) Japanese group co-spokesperson

Table 6: International cooperation in E06 (TREK)

Country	Institutions	Responsibility	Base institute
Canada and U.S.A.	ISU, U.Saskatchewan, UBC/TRIUMF, USC	Target	TRIUMF shop
U.S.A.	MIT	GEM chambers	MIT
Russia	INR	CsI(Tl)	INR and KEK
Japan	Osaka U., KEK etc.	Polarimeter	KEK

- MIT has recently established a GEM laboratory to perform R&D on GEM detector for the planned upgrade of the STAR detector at RHIC. We propose to utilize and extend the present R&D activity at MIT to develop the cylindrical C0 and planer C1 for E06 (TREK). Such a strategy of combining the R&D efforts has the great benefit of synergistic effects where expertise and effectiveness can be enhanced.
- INR is involved in many experimental projects such as CMS at CERN and HADES at GSI. The E06 INR group has close the contact with the people of these experiments. They will be responsible for the CsI(Tl) readout with APD. Our CsI(Tl) calorimeter will become the second application of APD readout to high energy experiment calorimeter next to CMS. The old INS group took responsibility for the E246 CsI(Tl) calorimeter. A. Ivashkin of this group is now responsible for the new system.
- Natural Science University in Ho Chi Mihn City is now eager to join the J-PARC activity. They sent a young scientist to the collaboration meeting in February'07. We regard it as very important to start such a collaboration with Asian countries at J-PARC.
- Other parts of the detector upgrade will be done by the Japanese group. They are the active polarimeter, the muon magnet and data acquisition. Several university people are now actively working for E06 (TREK).

We hold group meetings regularly, once a year at KEK and once a year outside of Japan. The first meeting abroad was held in November, 2006 at MIT (USA), The next meeting will be held in Saskatoon (Canada) in August, 2007.

5.3 Policy for funding

The cost of E06 (TREK) was re-evaluated for the FIFC report and the breakdown is listed in the report [1]. They are not very different from what we presented in the proposal. They are[5]:

(1) Detector upgrade cost	**279,710 kYen**
(2) Transfer of the spectrometer	**182,000 kYen**
(3) K1.1-BR branch construction	**50,000 kYen**

[5]The number for the transfer of the spectrometer was revised on June 26, 2007, because a wrong number 232,000 kYen was mistakenly given in the original version.

Table 7: Policy for funding

Item	Amount (kYen)	[Application to] or [budget source]
K1.1 upstream section	700,000-800,000	J-PARC operation money
K1.1BR branch part	50,000	Budget request in Canada incl. this cost
Transfer of spectrometer	182,000	KEK or J-PARC money
Target	some fraction	Fund application from a US university
Electronics	some fraction	Pool electronics for common use
Detector elements	about 270,000	Grant-in-Aid or J-PARC exp. money

It is anticipated that KEK will assume responsibility for the transfer of the spectrometer system, as it will become a general J-PARC facility like SKS. Also, the installation of the K1.1 upstream section (700-800 MYen including the preparation of intra-structure such as electricity power and cooling water), a general purpose beamline of J-PARC, will be the responsibility of J-PARC. It is desired that the beamline should be installed using the J-PARC operation money.

The funding scenario for the E06 (TREK) experiment is summarized in Table 7. The Japanese group plans to apply for Grant-in-Aid support money. Since we submitted the proposal, the University of Saskatchewan's administration is providing a lot of support to the Canadian team in applying for the major grants, conference funds. The American collaborators are also exploring their funding sources. Our collaborators have also found monies to support students to engage in short-term R&D work and to participate in collaboration meetings. A stage-2 approval from the J-PARC committee is highly desired, if not a pre-requisite, for the North American funding applications to be successful.

5.4 Policy for beam line construction

E06 (TREK) will use a low-momentum separate beam at K0.8 as the short branch of K1.1. The beam optics of K0.8 was designed by J.Doornbos at TRIUMF a member of the E06 (TREK) group. The K1.1 line along with its branch line K1.1-BR were included in the grand floor plan of the phase-1 Hadron Hall, which had been made by the J-PARC facility group and was endorsed by the first PAC meeting. K1.1-BR uses the upstream part of K1.1 with the first electric separator (ESS) with its configuration unchanged. Thus, the construction of K1.1-BR has been considered to be dependent on the K1.1 schedule regarding its beam optics, time schedule and funding.

The construction of the K1.1 beamline is, however, is included neither in the J-PARC construction budget nor in the experiment preparation budget of KEK. This is a very unlucky situation for the E06 (TREK) experiment, and it is due to underfunding of the total J-PARC construction budget. We cannot do anything. Now we strongly request that K1.1 (or at least its upstream part) should be constructed using the J-PARC operation money which will start in 2010 or by an independent budget request to the ministry.

While the K1.1 line with the total length will be used by general users in the future, the K1.1-BR is a dedicated beamline for the stopped kaon beam, *i.e.* for the E06 (TREK) experiment for the moment. The Canadian E06 group is considering a contribution to the leg of the channel and it is now preparing a funding request to be submitted this fall. A prerequisite for such a request is that the K1.1 upstream part should be funded by KEK. The components, B3, Q7, Q8 and an HFOC collimator amounts the cost of 50 MYen by making full use of recycled elements. (The total cost of K1.1 upstream is estimated to be 700-800 MYen including the infrastructure preparation.)

In order that the J-PARC facility group can proceed with the concrete planning of K1.1-BR and the KEK can provide a funding prospect we believe that a recommendation from the PAC for the early installation of this beamline is essential. We request the PAC to make a quick decision. The condition of the availability of a beam for a proposal to go to Stage-2 approval is now meaningless, because the condition of Stage-2 approval can also facilitate the beamline construction. This is the thinking of E06.

6 Conclusion

In this report we have tried to answer the questions raised in the first PAC meeting last year, and we hope that this had been done satisfactorily. In summary, we showed in a Monte Carlo simulation of the active polarimeter that a final statistical sensitivity of $\sigma(P_T) = 1.2 \times 10^{-4}$ should be obtained even using only the conservative analysis of the integral method of only fwd/bwd π^0 regions (Table 8). One change of prerequisite conditions is the 40% longer run time due to the reduction of the K1.1BR beamline acceptance; The K^+ beam intensity is now 70-75% lower than the previous estimate presented in the proposal. A further careful study of the systematics may enable us the use of π^0 $left/right$ events and the application of the event-by-event weighted analysis. Then a statistical sensitivity of better than 1.0×10^{-4} will be reachable.

We also showed that the most dangerous systematic error which is inherent in this kind of P_T experiment with a stopped beam now becomes controllable. The misalignment of the polarimeter and the muon field distribution, especially their rotation components ϵ_z and δ_z were the troublesome systematics in E246 because they could not be cancelled out by the π^0 fwd/bwd subtraction scheme. This situation does not change if we employ the same analysis. However, it was shown in this report, that an analysis using the spin direction (θ_0) information removes the ϵ_z effect and also decouples the δ_z effect from the real P_T effect, enabling the determination of P_T unbiased by a spurious effect. Other sources of systematic error are easy to control.

For this past year we have done our best to approach the final detailed design of the detector upgrade. By pinpointing the essential points we performed several test measurements. We can now proceed with the detector upgrade preparation. As was mentioned before, the Canadian and American people are starting budget requests in their countries.

Table 8: Summary of experimental sensitivity

	δP_T	Condition etc.
Statistical error	1.2×10^{-4}	fwd/bwd integral analysis
	1.0×10^{-4}	inclusion of $left/right$, needs more MC
Systematic error	$\preceq 1.0 \times 10^{-4}$	See Table 3

We would like to request the PAC to recommend to the IPNS and J-PARC administration that the E06 (TREK) experiment be considered for stage-2 approval without funding yet in place. The PAC might also strongly recommend to management that they provide prospects for financial resources such as the J-PARC operation money (in particular for the spectrometer transfer, the construction of the K1.1 beamline upstream part, and the detector construction cost when Grant-in-Aid money is not available in the near future) and to help the E06 (TREK) collaborators secure funds from other sources.

References

[1] FIFC E06 repor, June 2007; http://www-ps.kek.jp/e06/FIFC/E06_report.pdf

[2] M. Abe *et al.*, Phys. Rev. D**73**, 072005 (2006).

[3] J.Doornbos, April 2005,
http://trshare.triumf.ca/∼trjd/kstopbeam_jparc.pdf

[4] J.Doornbos, May 2007,
http://trshare.triumf.ca/∼trjd/koudolong.pdf

A Appendix : MC simulation of alignment calibration

In this Appendix supplemental explanations to the Monte Carlo simulation study of the polarimeter alignment in Section 3 are presented individually.

A.1 Monte Carlo code for positron asymmetry due to misalignments

The purpose of Monte Carlo (MC) studies is to show the principal ability of a unique determination of the misalignments of the polarimeter using $K_{\mu 3}$ events when several misalignments are existing simultaneously, and to determine the statistical accuracy of this experiment. A simulation program based on a GEANT3 code was used. The 2mm thick stopper plates with 6mm gap (31 plates in total) and a muon holding field were installed in the existing E246/470 simulation program. The spin relaxation is discarded and the spin holding field is uniform (30 mT) in the azimuthal direction. The stopper material is aluminum and no mechanical deformations were assumed. Although the muon stopping plate should be determined from an exact chamber analysis, we chose the plate here by following the muon track in the simulation. The e^+ direction was identified by the e^+ path in the adjacent gap of the muon stopped plate (the chamber efficiency is 100%).

In the real calibration measurement using actual data, we have to take into account the more detailed polarimeter structure and the positron detection characteristics with high enough statistical accuracy. However, the basic methodological performance of the calibration can be regarded to be proved in the present analysis. The muon field magnet design is now under way, and its real field strength and distribution might be slightly different. We regard 30 mT as the lowest value providing the safest result in the present study.

Among the possible global misalignments of the three parallel displacements and three rotations: the parallel displacements should not play a role as long as the active stopper covers the whole muon stopping region because of the parallel-shift symmetric structure. The rotation about the y-axis should not have an effect. Hence, the relevant global misalignments are:

- rotation of the active stopper around the r-axis: ϵ_r,
- rotation of the active stopper around the z-axis: ϵ_z.
- rotation of the muon field distribution around the r-axis: δ_r and
- rotation of the muon field distribution around the r-axis: δ_z.

Null test: The outline of the calibration procedures were described in the proposal, which we repeat here in more detail. The asymmetry of the muon decay positrons was calculated as

$$A = \frac{N_{fwd/left} - N_{bwd/right}}{N_{fwd/left} + N_{bwd/right}} \tag{20}$$

in the MC simulation for e^+ going in $fwd/back$ and $left/right$ directions under the condition of perfect alignment. The polarization was initially in the longitudinal direction lying in the median plane and precessing under the 30 mT field. The regions of fwd, bwd, $left$ and $right$ are defined appropriately. As is expected a precession pattern due to in-plane muon polarization is only observed in the e^+ fwd/bwd asymmetry.

When misalignments exist a small precession pattern appears in the e^+ *left/right* asymmetry. More generally, for an arbitrary initial muon spin phase in the median planes θ_0, as shown in Fig. 4, The time dependent asymmetry, A, can be expressed as:

$$\begin{aligned} A(\omega t, \theta_0) &= \alpha_0\{(\epsilon_r - \delta_r)\cos(\omega t - \theta_0) + (\epsilon_z - \delta_z)\sin(\omega t - \theta_0) \\ &\quad +\delta_r\cos\theta_0 - \delta_z\sin\theta_0\} + \gamma \end{aligned} \tag{21}$$

Here we add an additional offset term γ due to a possible asymmetric muon stopping distribution in the stopper or some unknown polarimeter defect such as chamber inefficiency. Rotation of the magnetic field generates the constant $\delta_r\cos\theta_0 - \delta_z\sin\theta_0$ term which mimics the actual T-violation effect and is rather crucial to ensure a precision of $\Delta P_T \sim 10^{-4}$.

Normalization: The initial polarization was assumed to be P_l, completely parallel to the K^+ beam direction ($\theta_0 = 0$) in the simulation. Fig. 8 shows the precession oscillation pattern of the *left/right* e^+ asymmetry with a finite misalignment of 1° rotation for one of the four ϵ_r, ϵ_z, δ_r, and δ_z misalignments while keeping the other rotations to zero. The precession patterns with the form of $\epsilon_r\cos\omega t$, $\delta_r(1-\cos\omega t)$, $\epsilon_z\sin\omega t$, and $-\delta_z\sin\omega t$ are observed. In the precession patterns, the asymmetry coefficient α_0 and the phases were determined. The fitted curves are also shown.

A.2 θ_0 determination for $K_{\mu3}$ events

The original muon spin direction was obtained from the kinematics of $K_{\mu3}$ decay products with a form of [1]

$$\begin{aligned} \vec{A} &= a_1(\xi) - a_2(\xi)[(m_K - E_\pi) + (E_\mu - m_\mu)(\vec{p}_\pi \cdot \vec{p}_\mu)/|\vec{p}_\mu|^2]\vec{p}_\mu \\ &\quad -a_2(\xi)\vec{p}_\pi + m_K m_\mu \mathrm{Im}(\xi)(\vec{p}_\pi \times \vec{p}_\mu), \end{aligned} \tag{22}$$

where

$$\begin{aligned} a_1(\xi) &= 2m_K^2[E_\nu + \mathrm{Re}(b(q^2))(E_\pi^* - E_\pi)], \\ a_2(\xi) &= m_K^2 + 2\mathrm{Re}(b(q^2))m_K E_\mu + |b(q^2)|^2 m_\mu^2, \\ b(q^2) &= 1/2[\xi(q^2) - 1], \\ E_\pi^* &= (m_K^2 + m_\pi^2 - m_\mu^2)/(2m_K). \end{aligned} \tag{23}$$

Here, the world average values of $K_{\mu3}$ form factors reported by PDG were used. The θ_0 value of each $K_{\mu3}$ decay at the muon stop position in the polarimeter was determined by taking into account the muon spin rotation by the spectrometer field. The muon spin direction was computed in the simulation using the relativistic spin transportation method [2]. Here we neglected the spin rotation by the B field of the spin holding magnet during the muon transportation. Fig. 9 (a) shows the θ_0 distribution for $K_{\mu3}$ events with the π^0 going forward (red) and backward (black). A significant overlapping region can be seen in the figure.

A.3 Determination of polarimeter misalignments

A Monte Carlo simulation was performed by assuming the misalignments of ($\delta_z = 5°, \delta_r = 0°$) and ($\delta_z = 0°, \delta_r = 5°$). The time-integrated e^+ *left/right* asymmetries ($A(\theta_0)$) were obtained as a function of θ_0, using Eq.(15) as shown in Fig. 9 (c) and (d). Black and red

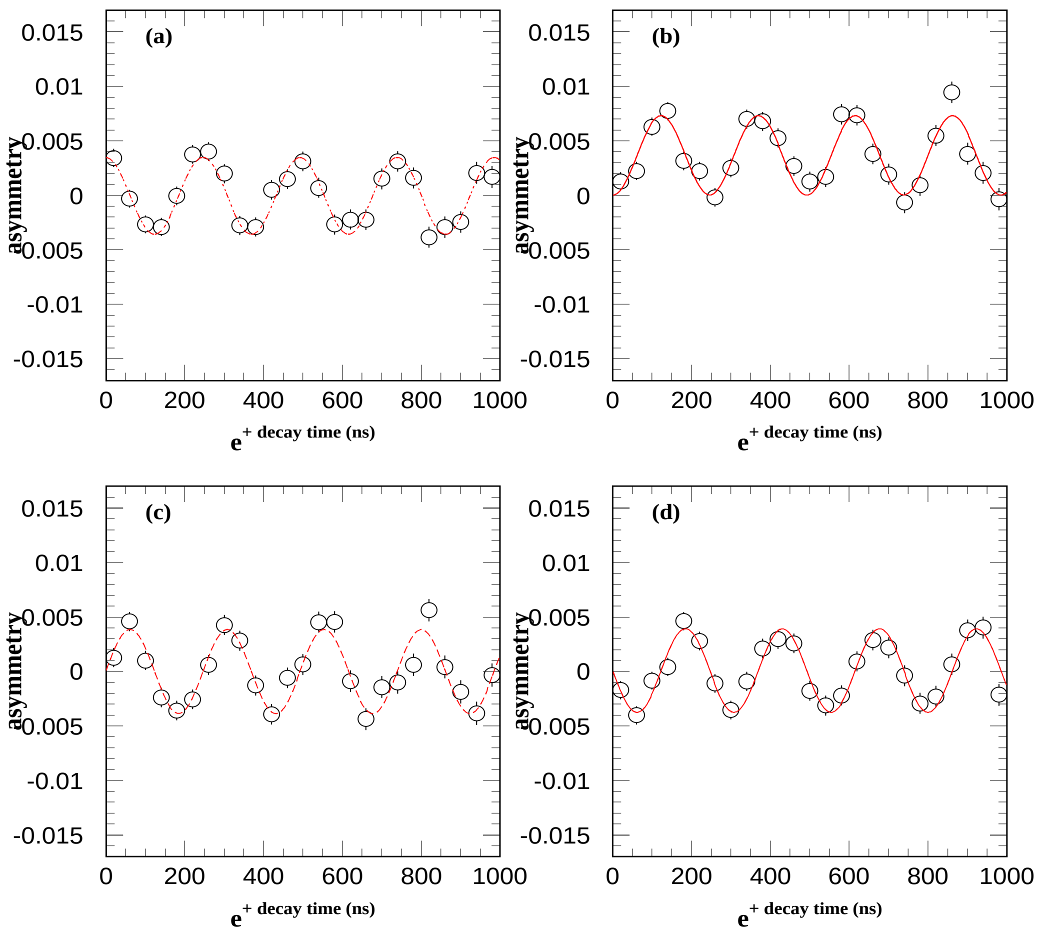

Figure 8: Left/right asymmetries with the finite misalignments of (a) δ_z, (b) δ_r, (c) ϵ_z, and (d) ϵ_r. One of four rotations was chosen by keeping other rotations to zero. Here, θ_0 was taken to be 0. Dotted lines are the fitted results. The precession patterns with the form of (a) $\epsilon_r\cos\omega t$, (b) $\delta_r(1-\cos\omega t)$, (c) $\epsilon_z\sin\omega t$, and (d) $-\delta_z\sin\omega t$ are observed.

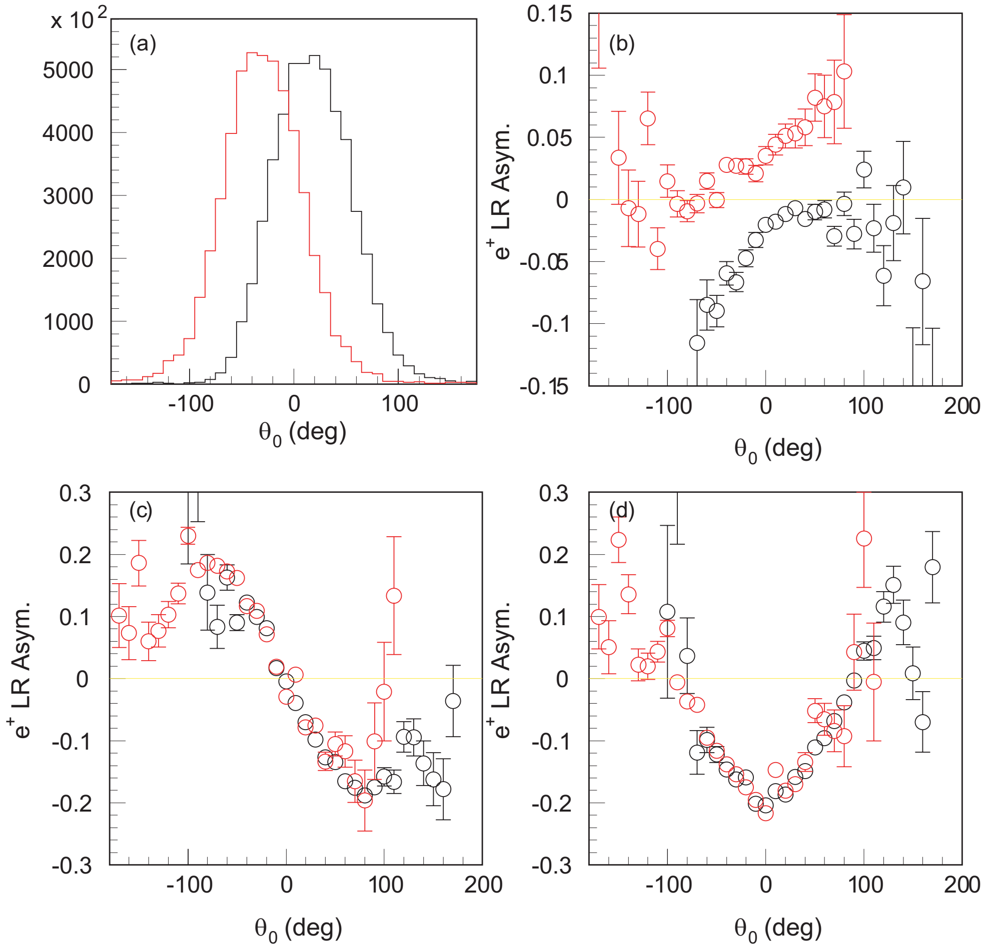

Figure 9: (a) $K_{\mu 3}$ θ_0 distributions and (b),(c),(d) e^+ *left/right* asymmetries as a function of θ_0 for events with π^0 going forward (red) and backward (black). The asymmetries were obtained with the assumption of (b) pure P_T, (c) $\delta_z = 5°$ and (d) $\delta_r = 5°$. The $A(\theta)$ values due to π^0 forward and backward events have positive and negative values, while $A(\theta_0)$ from the misalignments have a common θ_0 dependence.

circles are π^0 going forward and backward events, respectively. A T-violation effect was not considered here ($\mathrm{Im}\xi = 0$). Since the $A(\theta_0)$ distribution due to these misalignments can be describe as $A(\theta_0) = \delta_r \cos\theta_0 - \delta_z \sin\theta_0 + \eta(\theta_0)$ which depends only on θ_0, the $A(\theta_0)$ distributions for events with π^0 going forward(A_{fwd}) and backward(A_{bwd}) should have a common θ_0 structure. These θ_0 dependences were successfully reproduced by the MC simulation, as shown in Fig. 9 (c),(d).

As well as the misalignment effects, the P_T extraction procedure was studied as follows. Assuming a finite $\mathrm{Im}\xi$, the MC simulation was performed with $\delta_r = \delta_z = 0$. Using a manner similar to the above misalignment studies, the e^+ left/right asymmetry was determined as a function of θ_0. Fig. 9 (b) shows the calculated $A(\theta_0)$ distributions, showing different θ_0 structure for π^0 going forward (black) and backward (red) events. The $A(\theta_0)$ values due to the forward and backward events have positive and negative values, respectively, in the entire θ_0 region, while $A(\theta_0)$ from the misalignments have a common θ_0 dependence. Therefore, δ and P_T can be individually determined by adding and subtracting A_{fwd} and A_{bwd} for each θ_0 bin.

$$A_{sum}(\theta_0) = (\bar{A}_{fwd}(\theta_0) + \bar{A}_{bwd}(\theta_0))/2 \tag{24}$$
$$A_{sub}(\theta_0) = (\bar{A}_{fwd}(\theta_0) - \bar{A}_{bwd}(\theta_0))/2. \tag{25}$$

A_{sub} and A_{sum} are π^0 fwd/bwd double ratio analysis and null asymmetry analysis, respectively for each θ_0 bin. The results of the MC simulation are shown in Fig. 5(a) for A_{sum} and Fig. 5 for A_{sub}, indicating good separation of P_T, δ_z, and δ_r. The P_T and δ values were obtained by making error weighted average over the entire θ_0 region (A_{sub}^{av}, A_{sum}^{av}).

Assuming the existence of both $\mathrm{Im}\xi$ and δ at the same time, the above A_{sum} and A_{sub} analyses were repeated in order to check the validity of this analysis scheme. Fig. 5 (a),(b) show A_{sub} and A_{sum} distributions, respectively. The A_{sub}^{av} and A_{sum}^{av} values with the simultaneous existence of $\mathrm{Im}\xi$ and δ were compared with those with single $\mathrm{Im}\xi$ or δ case normalization as shown in Fig. 5 (c),(d). They are consistent within errors, indicating the validity of the $A_{sub}(A_{sum})$ scheme to cancel out the misalignments (T-violation) and extract the T-violation (misalignment) effect. Since P_T and δ contribute linearly to the e^+ $left/right$ asymmetry, the present analysis can provide a good separation between them.

A.4 Ambiguity of θ_0

Here we used the correct θ_0 values obtained by substituting true μ^+ and π^0 information into Eq.(23). However uncertainties from (a) finite detector resolutions and (b) errors in the $K_{\mu 3}$ form factors could degrade the asymmetry distributions in the actual analysis. To study the θ_0 uncertainty, θ_0 was calculated by using the observed μ^+ and π^0 information for (a) and by changing the $K_{\mu 3}$ form factors with $\pm 1\sigma$ level for (b). The distribution of θ_0 shift from its original value is shown in Fig. 10. Black and red histograms are for (a) and (b), respectively. The θ_0 resolutions were determined to be 2.4° from RMS values containing the tail part. Although these finite resolution have to be taken into account for the actual A_{sub} and A_{sum} analyses, the asymmetry distributions will not be strongly affected by this uncertainty and the systematic error due to this effect is less important.

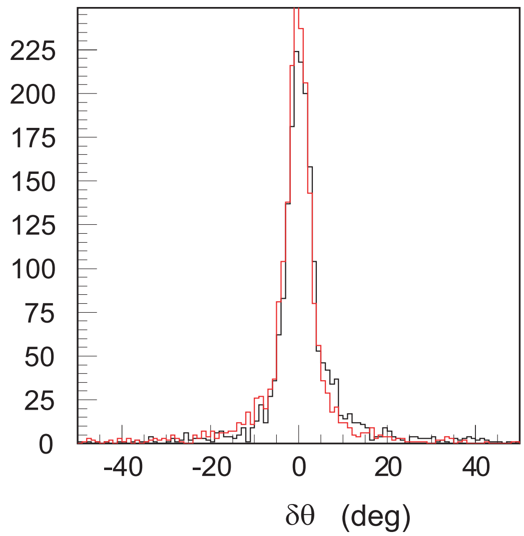

Figure 10: Distribution of $\delta\theta$, the shift of θ_0 from its original value, was calculated by using the observed μ^+ and π^0 information (black) and by changing $K_{\mu 3}$ form factors with $\pm 1\sigma$ level (red). The θ_0 resolution was determined to be 2.3°(black) and 2.4°(red).

References

[1] N.Cabibbo and A. Maksymowicz, Phys. Lett. **9**, 352 (1964).

[2] P. Depommier, KEK-E246 Technical Note No.28 (Internal).